Optical spectroscopy of highly ordered poly(p-phenylene vinylene)

1993 J. Phys.: Condens. Matter 5 7155

(http://iopscience.iop.org/0953-8984/5/38/011)

J. Phys.: Condens. Matter 5 (1993) 7155–7172. Printed in the UK

Optical spectroscopy of highly ordered poly(*p*-phenylene vinylene)

K Pichler†, D A Halliday†, D D C Bradley†, P L Burn‡§, R H Friend† and A B Holmes‡

† Cavendish Laboratory, Madingley Road, Cambridge CB3 0HE, UK
‡ University Chemical Laboratory, Lensfield Road, Cambridge CB2 1EW, UK

Received 19 July 1993

Abstract. We report a study of the photophysical properties of poly(*p*-phenylene vinylene), PPV, prepared in a way that gives an especially high degree of intrachain order. Optical absorption, photoluminescence, photoinduced absorption, and photoconductivity excitation spectra are presented and compared to data reported for less well ordered PPV. Spectral red shifts, sharpening of spectral lines, and a transfer of oscillator strength into the vibronic ground states of the electronic transitions are observed. Photoinduced absorption due to long-lived charged excitations, previously reported for less ordered PPV, could not be detected in this material. Photoconductivity excitation spectra show a steep rise at the absorption edge with no appreciable offset between the onsets for photoconduction and absorption. A very slow photocurrent component is observed, which we associate with the trapping and subsequent thermal release of photocarriers.

1. Introduction

Conjugated polymers form a very interesting class of electronic and optoelectronic materials with a wealth of potential applications [1, 2]. The chemical routes initially most widely used for synthesis meant, however, that most conjugated polymer samples had relatively large amounts of chemical impurities and chemical and structural defects present within them (e.g. catalyst residuals, sp^3 C atoms, irregularities in the coupling of monomer units, both static and dynamic structural defects such as chain bends and twists, etc). Recent advances in synthesis and processing have lead to dramatic improvements in both chemical purity and homogeneity. This, in turn, has given rise to improvements in the degree of order in the polymer films. The fact remains, however, that high-quality single crystals of these polymers are still not available (with the notable exception of the polydiacetylenes [3]). This has meant that investigations have had to be carried out on disordered, and at best polycrystalline, samples. In this situation, ascertaining whether the observed properties of conjugated polymers are intrinsic or are the result of defects and disorder becomes a difficult task. There is increasing evidence that some of the physical properties in conjugated polymers, in particular the nature as well as the static and dynamic behaviour of excited states, may be very closely related to the presence of such defects [4–8].

The conjugated polymer poly(*p*-phenylene vinylene), PPV, is of particular interest because it can function as the emissive layer in light-emitting diodes [9]; this device-related work has been made possible by the development of solution-processible precursor

§ Present address: Dyson Perrins Laboratory, South Parks Road, Oxford OX1 3QY, UK.

0953-8984/93/387155+18$07.50

polymers, including PPV, which can be converted *in situ* to form high-quality films of the insoluble conjugated polymer (see [10], and references therein). We briefly discuss the methods of synthesis of PPV in section 2 below, but mention here that we have recently found methods to improve the degree of intrachain order in this polymer to a large extent [11, 12].

We present here measurements of photophysical properties on this material, and find that the energetics and kinetics of the excited states are very much altered with respect to less ordered PPV. This provides us with important insights into the role of extrinsic factors in the photophysical properties of PPV. We can conclude that many aspects of what has previously been measured are controlled by disorder, probably in the form of chain bends and twists that limit the extent of straight chains. With the results presented in this paper we can address several important topics relevant to the modelling of electronic excitations in conjugated polymers such as PPV.

The semiconducting or conducting properties of conjugated polymers derive from the presence of π electron bands delocalized along the polymer chain. With partial oxidation or reduction, metallic levels of conductivity can be achieved. There has been a very high level of interest in the nature of the excited states, both charged and neutral. As a consequence of the low-dimensional electronic structure and weak interchain bonding, excited states take on the character of the molecular excitations, which are well studied in molecular crystals such as anthracene [13]. This molecular character is manifested in the localization of excited states to individual chains, and to localization within the chain. The character of these excitations has been modelled by several groups [14, 15]. Charged excitations are stable either as singly charged polarons, or (within one-electron models) as doubly charged bipolarons. These are commonly detected through the presence of sub-gap-induced optical absorption [14]. In PPV, for example, singlet and triplet excitations can be formed either by photoexcitation [16], or by electron-polaron–hole-polaron capture [9, 17, 18], and show clear evidence for spatial localization [19]. Radiative decay of singlet excitons can give efficient luminescence which has been extensively measured [9, 16, 20, 21]. Radiative decay of triplet excitons has not been observed, but optical transitions within the triplet manifold give rise to strong induced optical absorption [16]. Although the models used provide a good qualitative description of the excitations, there are several aspects that are not well understood. We mention below some of these that are relevant to the measurements that we present here.

1.1. Effective conjugation, extent of electronic wavefunctions, and vibronic coupling

The extent of straight planar chain segments, unperturbed by chain bends, twists, and other defects, is an important parameter in this study as it determines the extent of effective conjugation, or the effective conjugation length [14, 15]. This determines the energies of the electronic ground and excited states, and also the extent of the electronic wavefunctions. The spatial extent of the ground and excited electronic wavefunctions controls the Franck–Condon overlap integrals (via the difference in ground-state and excited-state geometries), which determine the strengths of the vibronic progressions in the electronic transitions in absorption and emission. From the strengths of these vibrational progressions, as measured in absorption and emission spectra, we can estimate the degree of localization of the excited states and we can estimate qualitatively the extent of geometric chain relaxation in the excited state. The strength of coupling between the ground- and excited-state geometries is normally modelled within the Franck–Condon model by the Huang–Rhys parameters [22]. In the case of PPV, the vibrational modes that couple most strongly are the ring-stretching modes with frequencies at around 1600 cm^{-1} [16, 23].

We use the following notation for electronic transitions in absorption and emission: $S_0 \rightarrow S_1/n \rightarrow m$ denotes a transition from the singlet ground state to the first excited singlet state ($S_0 \rightarrow S_1$) and between the nth vibrational level of S_0 to the mth vibrational level of S_1. T_1 and T_2 will denote the lowest triplet and next lowest triplet states, respectively. The triplet state T_1 in PPV is produced via intersystem crossing from the photoexcited S_1 [16, 19, 24].

The extent of conjugation in PPV has been investigated by making comparison with a series of well defined phenylene-vinylene oligomers [6, 25, 26] and PPV-based polymers [27, 28]. These studies give an estimate of around 15–20 phenylene-vinylene units as the longest unperturbed conjugated segments in this improved PPV (we note that this corresponds to chain lengths comparable to the intrachain coherence length determined from electron diffraction studies [11, 29].

A further process that limits the extent of effective conjugation in PPV, and conjugated polymers in general, is the temperature-induced excitation of vibrational, rotational, or librational modes of the chain. These temperature-induced excitations may also serve to localize the wavefunctions [22]. The combined effects of conjugation breaking and localization of wavefunctions can be seen in absorption and luminescence as a function of temperature. The low-frequency rotational and librational modes can couple effectively to the electronic transitions [28]. The issue of the influence of torsions on the energy of electronic levels has recently been investigated theoretically on phenylene-vinylene oligomers [30]. We note that there is clear evidence for the presence of such torsions in PPV chains from NMR, x-ray diffraction and neutron-scattering studies [31–34].

1.2. Stokes shift and self-localization

In standard PPV, a finite Stokes shift between the lowest-lying absorption ($S_0 \rightarrow S_1/0 \rightarrow 0$) and highest-lying emission ($S_1 \rightarrow S_0/0 \rightarrow 0$) has been observed [16]. However, this 'apparent' Stokes shift is largely due to spectral diffusion of photoexcited states to lower-energy segments (longer/better conjugated chain segments) [27, 35]. The remaining, intrinsic, Stokes shift after consideration of reflectivity (for the absorption spectra), self-absorption (for the emitted luminescence), and spectral diffusion, gives information about the phonons that couple to the electronic transitions. In an earlier study of the high-intrachain-order PPV investigated here, it was shown that the intrinsic Stokes shift in this material approaches zero [27]. Nevertheless, as mentioned in section 1.1 and discussed in more detail below, the coupling of absorption and emission to high-frequency intrachain vibrational modes indicates that there is chain relaxation in the excited state. This coupling to vibrationally excited states in absorption ($S_0 \rightarrow S_1/0 \rightarrow n$) and the subsequent relaxation to the vibrational ground state of S_1 (i.e. geometric chain relaxation and emission of phonons) produces the self-localized neutral polaron-exciton, within the description due to Fesser *et al* [36].

1.3. Binding energy of the photoexcited state

When a singlet exciton is formed after photoexcitation, there are several decay channels: radiative recombination, intersystem crossing to form a metastable triplet exciton (T_1), separation of the exciton to give two charge carriers of opposite charge, and diffusion to quenching sites where non-radiative recombination may occur. The rates for these different transitions obviously determine the luminescence efficiency and thus the efficiency in electroluminescent devices. They also determine, together with the exciton binding energy, the efficiency for charge separation, and hence photoconductivity [37–39]. Both

photoconductivity and luminescence are efficient processes in PPV and the balance is strongly influenced by the exciton lifetime [20,21,40], and the exciton binding energy. Recent theoretical [41] and experimental [42] studies have addressed this issue of the exciton binding energy in PPV. This has given values around 0.3–0.4 eV.

1.4. Charged excited states

Charges introduced in conjugated polymers by chemical doping are considered to be stored in the form of self-localized solitons, polarons, and bipolarons, with quantum states moved deep into the (ground-state) energy gap [14,15,36]. Although the effects of the dopant are not usually explicitly considered, it is very likely that the Coulomb interaction with the counterions plays an important role in the stabilization of the excited state, particularly for the double charged bipolaron [43]. Charges created by photoexcitation appear, however, to show the same characteristics as those introduced by doping. In the case of PPV, for example, a previous study on low-intrachain-order material has shown that photoinduced bipolarons are metastable and give rise to additional absorptions from/to these intragap states due to the self-localized bipolaron. However, there is now increasing evidence for various polymers that the stability of these self-localized charged states depends very much on the state of order, the presence of defects, and interchain coupling in the polymers [4–8,44,45]. In the present work, we find that the characteristics of the charged excitations are strongly altered from those produced in less ordered material.

2. Preparation of materials

Figure 1 shows the chemical synthesis routes to PPV (**5**) via (i) the sulphonium salt polyelectrolyte precursor, termed the 'standard' route (**1** → **2** → **5**), and (ii) our modified precursor route, termed the 'improved' route (**1** → **2** → **3** → **4** → **5**). In both routes a commercially available monomer (**1** in figure 1) is polymerized with a base to yield a sulphonium salt polyelectrolyte precursor polymer (**2**) ($a \gg b$). If tetra-*n*-butylammonium hydroxide in methanol is used as the base, a slightly better resolved vibronic structure is observed in the absorption spectrum than when NaOH is used [12]. The sulphonium salt precursor polymer **2** prepared by either base is converted to standard PPV by heat treatment in vacuum. Improved PPV is produced by additional treatment of the precursor **2** with the organic base in order to promote elimination of leaving groups and hence to increase the relative fraction of conjugated units in the precursor **3** ($d > b$). The sulphonium groups are then displaced by methoxy groups to give a partially conjugated methoxy-leaving-group precursor **4** which is soluble in chloroform. It has been shown that methoxy-leaving-group precursors give better ordered PPV than precursors with the larger sulphonium side groups [12,46]. The displacement reaction from **3** to **4** also promotes further elimination of leaving groups and the relative content f of conjugated phenylene vinylene units in the methoxy precursor($f > d$) increases up to about 40%, as assessed from the alkene-proton NMR [11]. The resulting partially conjugated methoxy precursor **4** is then converted to give improved PPV by thermal treatment, at temperatures of typically 220 °C, under an Ar gas stream containing HCl acid vapour as a catalyst.

In the following we refer to two different types of standard PPV (termed type I and type II). Type I refers to PPV prepared via the precursor polymer synthesized using NaOH as base and discussed in earlier publications [16]. Type II refers to material prepared using either NaOH or organic-base polymerization but for which we have refined and optimized the various synthesis steps and thermal conversion of the precursor polymer. Type-II

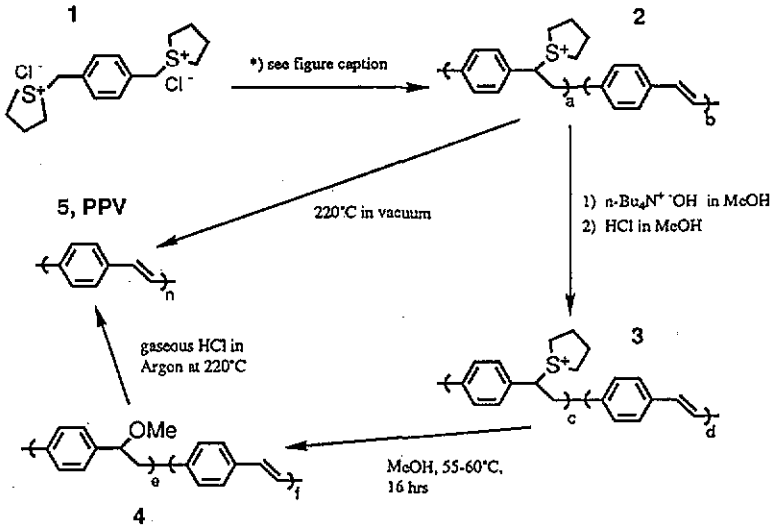

Figure 1. Chemical synthesis route to standard and improved PPV. *: step (1), polymerization with NaOH or n-Bu_4N^+ $^-$Oh in H_2O or MeOH, respectively; step (2), neutralization with HCl in H_2O for NaOH or HCl in MeOH for n-Bu_4N^+ $^-$OH; step (3), dialysis in H_2O for NaOH or in MeOH for n-Bu_4N^+ $^-$OH.

standard PPV is better ordered (lower energy gap and better resolved vibronic structure in the absorption band) than type-I standard PPV, and several consequent differences are observed as discussed more fully below. We mentioned above that the choice of base used for the polymerization makes a difference [12]; however, this difference is not pronounced and does not affect the photophysical properties reported for type-II standard PPV reported elsewhere in this paper.

The variations in the synthesis procedure are described in greater detail elsewhere [10]. The main change affected by these chemical modifications of the precursor polymer seems to be an increase in the relative number of stiff rod-like conjugated units in the precursor polymer. This introduction of a high relative content of stiff segments in the precursor will undoubtedly affect the processes involved in film formation and may bestow a partial mesogenic character. The introduction of stiff conjugated units in the precursor has very dramatic effects on the extent of conjugation in the improved PPV, the consequences of which are detailed below, and in several recent publications [11, 12, 46]. Electron-diffraction experiments indicate that PPV prepared via the improved route has an especially long (for spin-coated PPV) average intrachain coherence length of ~ 90 Å. This compares with ~ 50 Å for standard PPV [11, 29]. The interchain coherence length of the improved PPV is slightly less than that of standard PPV (45 Å versus 60 Å respectively). Thus we can visualize the improved material as having a high proportion of relatively extended unperturbed polymer sgements but with the registry between chains lost over a slightly shorter distance than in standard PPV. This degree of order still leaves much scope for improvement (e.g. in comparison with single-crystal polydiacetylenes [3]) and suggests that the conformations of polymer chains are likely to retain deviations from the calculated ideal (see [51] and references therein). What is striking though is that, as described below, even on length scales of the order of 15 repeat units, there are large changes in optical spectra. Experiments to obtain macroscopic ordering of improved PPV so as to enhance the interchain coherence and to assess the anisotropic properties are in progress [47].

3. Experimental details

The optical absorption of samples spin coated on spectrosil substrates and converted *in situ* was measured as $\log(T_0/T)$ in a Perkin–Elmer λ-9 UV–NIR–VIS spectrophotometer. Low-temperature absorption measurements were made at 77 K in a liquid nitrogen cryostat under dynamic vacuum, whilst room-temperature measurements were performed in air. The data have not been corrected for the effects of spectral variations in sample reflectivity. Some of the samples were not uniformly clear but rather showed slight opacity due to scattering. The effects of reflection and scattering are the main cause of the pronounced tail extending below the absorption edge as seen in the optical absorption spectra below. We note that the real part of the dielectric function, and hence the reflectivity, has peaks below the absorption peaks, which, if not corrected, increase the apparent absorption below the energy gap. The peak absorption, $\log(T_0/T)$, of the samples was in the range from 0.5 to 1.5.

Luminescence, photoinduced absorption, and photoconductivity were measured with the samples mounted in a He-flow cryostat at temperatures down to 10 K. Luminescence spectra have not been corrected for the spectral response of the detection system. Photoinduced absorption measurements employed two monochromators in order to prevent optical pumping with the probe beam and to cut out the pump light from the signal. A W lamp was used as the probe source and mechanically chopped pump light was provided by various visible lines from an Ar-ion laser (mostly the 457.9 and 488 nm lines). We used Si and InAs solid-state detectors, depending on the spectral range. Luminescence and photoinduced absorption were measured as a function of temperature, chop frequency, and pump intensity. A two-phase lock-in amplifier was used in order to separate signal components that have different characteristic decay times.

For photoconductivity measurements the PPV films were prepared on quartz substrates onto which interdigitated Au electrode arrays had been previously deposited (electrode separation of 7 μm and electrode width 24 cm). The pre-monochromated W lamp (used as the probe beam in photoinduced absorption) was used as an excitation source. Intensity dependence measurements and data calibration were made with the 488 nm line of the Ar-ion laser using neutral-density filters to vary the intensity and measuring the power with a calibrated power meter. Most photoconductivity measurements were performed in steady state, i.e. current readings were taken after the signal settled to a value within less than 5% of the equilibrium value. Due to the high resistivity of our PPV and the in-plane geometry of the devices very low currents had to be measured. This, together with the presence of trap states, results in long time constants, so that dynamic measurements cannot be performed easily. A Keithley 237 source/measure unit was used as voltage source and electrometer. For the photoconductivity excitation spectrum constant fields in the range from less than 10^4 up to 10^5 V cm^{-1} were applied. The samples were illuminated from either the front or the back (electrode) side. The photoconductivity excitation spectra were normalized to constant incident intensity; reflection was not corrected for. Typical dark conductivities at room temperature were of the order of 10^{-12} S cm^{-1}. The photoconductivity signal is instantaneous within the time resolution of our apparatus ($\sim$ 0.5 ms) and the response is very large; from this and the temperature dependence of the dark conductivity and photoconductivity we can exclude the presence of any significant heating effects when using pump light above the energy gap. Further information on the experimental parameters is given as necessary below.

4. Optical absorption and photoluminescence

4.1. Results

Figure 2 shows the optical absorption spectra of standard (type-II) and improved PPV at room temperature plus the spectrum of the improved PPV sample at 80 K. Note that the type-II material shows better resolved vibronic structure and a lower π–π^* energy gap (indicative of the higher degree of conjugation) than the type-I material [16,48]. The samples in figure 1 have peak values of absorbance of around unity and, for easier comparison, all spectra have been normalized to the same peak value. As discussed above, the long tails extending to lower energies are due to the effects of both scattering and uncorrected reflectivity.

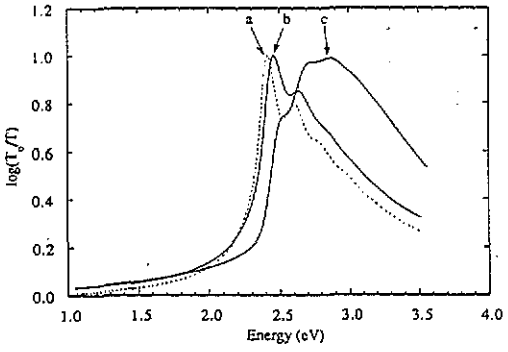

Figure 2. Optical absorption of improved (curve a, 80 K; curve b, room temperature) and type-II standard (curve c, room temperature) PPV, measured as $\log(T_0/T)$. The spectra are not corrected for reflectivity.

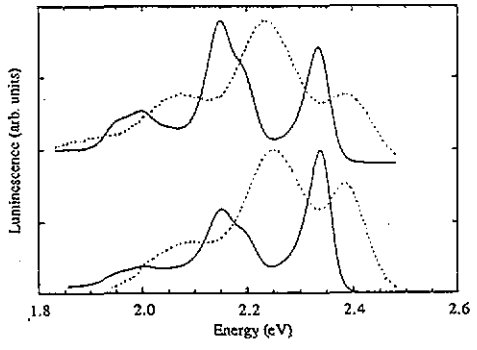

Figure 3. Luminescence spectra of improved PPV (bottom curves) and type-II standard PPV (top curves, displaced for clarity). Full curves show the spectra at ~ 15 K and broken curves show the spectra at room temperature. All spectra are normalized to the same peak value. The samples were excited at less than 40 mW cm^{-2} at 2.7 eV.

Our best sample of standard PPV shows limited vibronic structure; the $S_0 \rightarrow S_1/0 \rightarrow 0$ transition is at roughly 2.55 eV and the maximum of absorption is at 2.85 eV ($S_0 \rightarrow S_1/0 \rightarrow 2$). These energies are lower and the structure in the absorption is better resolved than reported previously for type-I standard PPV [16,48]. The spectra of improved PPV show an especially well resolved $S_0 \rightarrow S_1/0 \rightarrow 0$ transition. To our knowledge a better resolved $S_0 \rightarrow S_1/0 \rightarrow 0$ peak in conjugated polymers has so far only been reported for single-crystal polydiacetylenes [3] and a vapour-deposited isoelectronic analogue of PPV, namely poly(1,4-phenylenemethylidynenitrilo-1,4-phenylene-nitrilomethylidyne), $(C_6H_6\text{–}N{=}CH\text{–}C_6H_6\text{–}CH{=}N)_n$ [49]. Note that for our samples of improved PPV, there is no chain alignment within the plane of the film since the random

orientation inherent in the spin-coating film deposition is maintained (in contrast to the gel-drawn polyethylene poly[2-methoxy,5-(2′-ethyl-hexyloxy)-*p*-phenylene vinylene] (MEH-PPV) blends investigated by Hagler *et al* [22, 50], in which good intrachain order is achieved only through gel drawing). In addition, the peak absorption of the improved PPV is red shifted from that for type-II standard PPV, with the $S_0 \rightarrow S_1/0 \rightarrow 0$ transition at 2.463 eV at room temperature and at 2.416 eV at 80 K (there is very little further red shift on lowering the temperature from 80 K to 10 K) [51]. The room-temperature and 80 K absorption spectra of improved PPV in figure 2 indicate that there is little increase in the resolution of the vibrational sidebands on cooling, and little change in Franck–Condon factors for the vibronic transitions.

Luminescence spectra for both standard and improved PPV at both room temperature and ~ 15 K are shown in figure 3 (all spectra are normalized to the same peak value and the standard and improved PPV spectra are displaced for clarity). We note that the energies of the emission peaks and their vibronic progression in the two forms of PPV are almost identical at both temperatures. Self-absorption of the emitted light close to the absorption edge may cause an apparent shift of the peak position of the $S_1 \rightarrow S_0/0 \rightarrow 0$ transition. However, for the peaks that are not affected by self-absorption we find that the energy difference between the low-temperature $S_1 \rightarrow S_0/0 \rightarrow 0$ transitions of standard and improved PPV is less than 5 meV, whilst that between the $S_1 \rightarrow S_0/0 \rightarrow 1$ transitions of standard and improved PPV, at both low and room temperatures, is less than 10 meV. There is some slight sample-to-sample variation, but the 5 and 10 meV energy differences are the upper limits. That the emission energies are so similar indicates that there is very little difference between the most fully conjugated segments in the two different forms of PPV.

The red shift of the $S_1 \rightarrow S_0/0 \rightarrow 0$ emission on going from room temperature to 10 K is about 50 meV, much the same as in the absorption spectrum. The temperature shift of the peak in emission for the $S_1 \rightarrow S_0/0 \rightarrow 1$ transition is about 85 meV for standard PPV and 95 meV for improved PPV. The separation, at 10 K, between the $S_1 \rightarrow S_0/0 \rightarrow 0$ and $S_1 \rightarrow S_0/0 \rightarrow 1$ peaks in emission is about 190 meV for standard PPV and 185 meV for improved PPV (cf 180 meV in absorption at room temperature and 195 meV at 80 K for improved PPV) [23]. As is obvious from figure 3, there is at least one other vibrational mode involved in the $S_1 \rightarrow S_0/0 \rightarrow 1$ transition (shoulder). Note that, as also reported for MEH-PPV [22], the vibrational frequencies are softer for emission than for absorption. The temperature dependences of the emission peak positions and intensities are shown in figure 4 for improved PPV. The position and strength of the peaks are roughly constant from the lowest temperatures to about 50–60 K; above this temperature the peaks blue shift and the intensity decreases. The integrated emission intensity falls by a factor of between 3.0 and 3.5 between 10 K and 300 K for both the standard and improved PPVs.

4.2. Discussion

The increased order that is present in the improved PPV brings about very substantial changes in the character and distribution in energy of the singlet exciton. There are several aspects of the results obtained here that give interesting perspectives on the semiconductor properties of these materials.

The difference between the standard and improved PPV absorption spectra in figure 2 is, we believe, due to the weighting of different lengths in the conjugation-length distribution. In improved PPV, the distribution appears to be heavily weighted towards long conjugation lengths whilst in standard PPV samples there is a heavier weighting of shorter conjugation lengths. As mentioned in section 1.1, comparison with oligomers indicates that conjugation

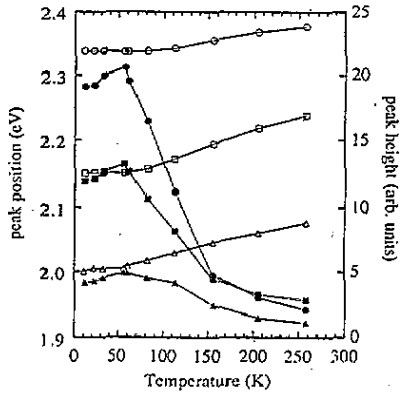

Figure 4. Peak energies (open symbols; left axis) and intensities (filled symbols; right axis) of the three resolved luminescence peaks in improved PPV as functions of temperature. Sample and experimental parameters are as in figure 3.

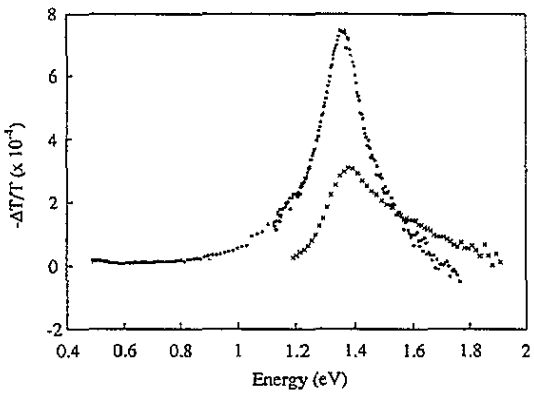

Figure 5. Normalized photoinduced absorption of improved PPV (dots) and type-II standard PPV (crosses); both at 15 K, 2.71 eV pump energy at less than 40 mW cm^{-2} incident pump intensity; improved PPV at 67 Hz chop frequency and standard PPV at 213 Hz. The difference in peak intensity between the two samples may not be significant, due to different pump/probe alignment and different pump power actually absorbed in the samples (different film thicknesses).

lengths range up to about 20 repeat units [6]. The variation in conjugation length is the principle cause of the inhomogeneous broadening of vibronic lines in the absorption spectra.

As with the standard PPV, emission spectra show better resolved structure than the absorption spectra, and this is now well established to arise from spectral diffusion within the range of accessible singlet exciton states produced by photoexcitation. Spectral diffusion involves migration of the excited states to the lowest-energy (i.e. most conjugated) polymer chain segments prior to their radiative decay and consequent emission [27, 35]. Emission spectra thus sample only the most conjugated segments of the polymer chains. Absorption spectra, however, contain contributions from all polymer chain segments; absorption occurs instantaneously and thus samples the distribution of conjugation lengths in its totality. We note that the spectra in emission for the two forms of PPV are very similar, in contrast with the absorption spectra for the same samples. This demonstrates clearly the effect of efficient spectral diffusion. The time evolution of the emission spectra might however reveal differences in the two types of PPV, and such measurements are in progress [20].

Although the vibronic structure in both emission and absorption is clearly resolved, a detailed study of the vibronic progression using a Franck–Condon analysis is hampered by the coupling of more than one vibrational mode. The presence of at least two different vibrational modes that couple to the electronic transition gives rise to an increased broadening of vibronic lines with increasing vibrational quantum number; the higher-order modes of each vibration become increasingly separated in energy (see the $S_1 \rightarrow S_0/0 \rightarrow 1$ and $S_1 \rightarrow S_0/0 \rightarrow 2$ transitions in figure 3). The $S_1 \rightarrow S_0/0 \rightarrow 0$ transition is much narrower than the vibrational progression of 0–1 and 0–2 lines. For these reasons we have not performed a Franck–Condon analysis. It is nevertheless evident qualitatively that the vibronic progressions in the spectra in figures 2 and 3 demonstrate that the coupling of electronic transitions and vibrational modes is significantly reduced in better ordered samples, at all temperatures; in going from standard PPV to improved PPV the relative strength of the 0–n (vibrational quantum number $n = 1, 2$, etc) transitions is decreased. This is indicative of a decrease in the offset in configuration coordinate between the ground-

and excited-state potential surfaces. The latter could be rationalized either as a result of a reduction in the anti-bonding character of the excited state, possibly through extension of the electronic wavefunctions, or as a result of a reduction in disorder-related internal forces that affect the configuration coordinates of the ground- and excited-state potential-surface minima. Other possibilities may exist and we are unable at this stage to give a fuller explanation of this behaviour.

Both the electronic energy gap between S_0 and S_1 and also the Huang–Rhys factors depend on the effective conjugation length, but appear not to show the same dependence. Our results indicate that the Huang–Rhys parameter is rather more sensitive to changes in conjugation length at high levels of order than the singlet energy gap. Note, for example, that the emission energies for standard and improved PPV, as shown in figure 3, are the same, but that the relative weights of the Franck–Condon factors are significantly different.

We observe that the blue shift in emission on warming from low temperatures to room temperature does not produce a large change in the Franck–Condon factors, in contrast to the case of MEH-PPV for which it has been argued that in a quasi-one-dimensional conjugated polymer system any reduction in the state of order (as measured by the blue shift of the emission) will cause an increased localization of the excited-state wavefunctions [22]. We consider that the difference between these two materials is that there are additional modes for thermal excitation in the MEH-PPV embedded in the polyethylene matrix.

The increased sharpness of the absorption and emission features over the standard PPV allows more detailed analysis of the spectra than previously possible. As has been reported previously [27], the Stokes shift between the $(0 \rightarrow 0)$ absorption and emission lines approaches zero for the improved PPV; without correction for self-absorption and reflectivity we measure a value here of about 80 meV between the peaks in emission and absorption. Spectral diffusion accounts for much of this value [27].

Energies between vibronic transitions can be determined with some precision. We note that the spacing between the $S_0 \rightarrow S_1/0 \rightarrow 0$ and $S_0 \rightarrow S_1/0 \rightarrow 1$ transition is about 180 meV (1450 cm^{-1}) at room temperature and about 195 meV (1570 cm^{-1}) at 80 K. This reduction in energy on increasing the temperature has been reported also for MEH-PPV and is discussed by Hagler *et al* [22]. Similar behaviour might be anticipated for PPV since the relaxation of excited states involves vibration of the polymer backbone, which is basically the same for both PPV and MEH-PPV. Some caution is however required in reading much into these results since there are clear indications that more than one vibrational mode couples to the electronic transition. This can be seen more clearly in the luminescence spectra for both standard and improved PPV at both room temperature and $\sim$ 15 K, shown in figure 3. We also note that a previous study on a derivative of PPV with methoxy side groups showed no change of the energies of the vibrational modes with temperature [5].

We consider that the red shift with cooling, observed both for absorption and emission, is qualitatively explained by the freezing out of torsional modes that act to decrease the coplanarity of the phenylene rings along the chain and hence reduce the π and π^* bandwidths. Recent experiments on PPV and theoretical investigations on the influence of ring torsions on the molecular energy levels of model oligomers indicate that activation of torsional modes is a plausible explanation of this behaviour [30–34]. We note also that the temperature at which this thermal shift of the emission sets in, $\sim$ 60 K (figure 4), is also the characteristic temperature above which there is thermal broadening of the emission peaks, and above which the intensity (and lifetime) of the singlet and triplet excitons (see section 5 below) starts to fall. It is likely that thermal activation of these modes is responsible for all these phenomena, since these torsional modes are the lowest-energy vibrational modes that couple effectively to the π-electron system.

5. Photoinduced absorption and photoconductivity

5.1. Photoinduced-absorption results

Figure 5 shows the spectrum of photoinduced absorption of improved PPV and also type-II standard PPV. The small luminescence background in this spectral range has been subtracted from the signal shown. The photoinduced absorption response was measured over a wide range of temperatures, chop frequencies, and pump intensities. For both types of sample, we were unable to detect any response, within the resolution of our experimental set-up ($-\Delta T/T \geqslant 5 \times 10^{-6}$), other than that at 1.36 eV (for improved PPV) and at 1.38 eV (for standard PPV); this peak is readily assigned to a triplet–triplet absorption. This peak has previously been observed at about 1.45 eV (type-I standard PPV) [16] and the red shift in improved and type-II standard PPV in figure 5 is in agreement with the red shifts of the other optical transitions, see section 4. In particular, no transitions could be detected at 0.6 or 1.6 eV, where peaks have been observed previously in some samples of standard PPV and assigned to the presence of photogenerated bipolarons [16, 24]. The measurement of the photoinduced absorption with the experimental system used here, see section 3, is very sensitive to the lifetime τ of the photoexcitations. Where this lifetime is considerably less than the inverse chop frequency $1/\omega$, the measured response is proportional to τ, and where τ exceeds $1/\omega$, the measured response falls as $1/\tau$ [16]. The response associated previously to bipolarons showed that the dynamics of the decay for these samples of PPV was strongly dispersive, with long-lived components of the decay greater than 100 ms at low temperatures. The absence of a similar response in both the type-II standard PPV and also in the improved PPV indicates that the combination of the generation rate of such excitations and the decay kinetics strongly reduces the photoinduced-absorption response. We consider that the principal factor is a reduced generation rate of these excited states.

The triplet–triplet absorption in figure 5 for the highly ordered PPV is symmetric, as also is the equivalent transition in the PPV oligomers, although these also show a low-energy feature due to several extra transient absorption features [6]. The same peak in standard PPV, both type I and type II, is asymmetric, with a strong tail on the high-energy side, as seen in figure 5 for type-II standard PPV. This has previously been assigned to the presence of a distribution of less conjugated segments. If, however, we assume that the triplet states (produced from singlet excitons via intersystem crossing) are mobile and subject to spectral diffusion as in the case of luminescence, we should not see a difference in the triplet–triplet absorption of standard and improved PPV. We can understand the observations if the triplet states are much less mobile than the singlet excitons (expected since triplet excitons can only transfer between chains by tunnelling) so that spectral diffusion is not complete, certainly for standard PPV, as evident from the tail on the high-energy side of the absorption for standard PPV in figure 5.

We show the temperature dependence of the triplet–triplet photoinduced-absorption responses for both improved PPV and type-II standard PPV in figure 6. At low temperatures the signal is of comparable strength in type-I and type-II standard PPV and in improved PPV. The response decays very quickly with increasing temperature and is not readily discerned from noise above about 70 K for both improved and type-II standard PPV. We have recently measured photoinduced absorption on a type-II standard PPV sample that was slightly less ordered (as assessed from optical absorption) than the standard PPV used for the studies here and shown in figure 2 [17]. In that sample the triplet–triplet absorption was asymmetric and the signal decreased by a factor of about 300 from 10 K to 60 K; above 60 K the signal was not readily detectable. This is in contrast to what has been reported for type-I standard PPV by Colaneri *et al* [16], who found that the triplet signal was observable up to about 150 K.

This may indicate that triplet states in improved PPV and higher-quality standard PPV are less strongly pinned and more mobile and therefore undergo triplet–triplet collisions more easily [18, 19]. We notice that the temperature at which the triplet photoinduced absorption vanishes in improved PPV coincides with the temperature at which the luminescence intensity and peak positions start to change (see section 4 above).

We have also investigated the frequency dependence of the triplet–triplet transition. This is shown in figure 7 for improved PPV at three temperatures (10, 30 and 50 K). The luminescence response is also shown, to provide an indication of the system response (its lifetime in PPV is typically less than 250 ps at room temperature [20]). The triplet response falls at high frequencies, and from the transition region between constant and decreasing signal in figure 7 we obtain lifetimes of $\sim$ 1 ms at 10 K and $\sim$ 0.25 ms at 50 K. The corresponding lifetimes in type-I standard PPV have been reported as $\sim$ 1 ms at 37 K (with no change at temperatures below) and $\sim$ 70 μs at 100 K [16].

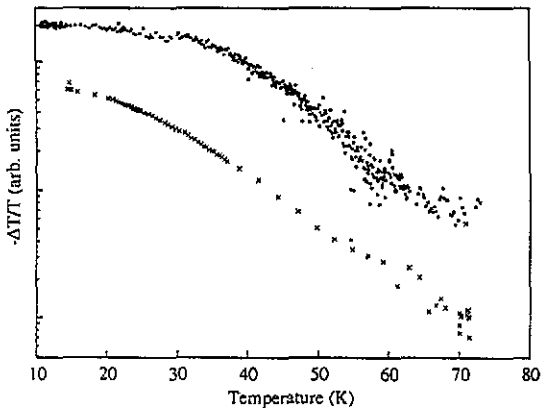

Figure 6. Temperature dependence of the peak signals of figure 5: dots denote improved and crosses the standard PPV.

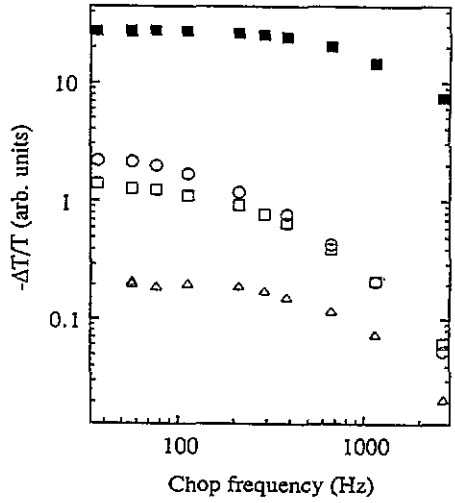

Figure 7. Chop-frequency dependence of the $S_1 \rightarrow S_0/0 \rightarrow 0$ luminescence peak of figure 3 (filled squares, 10 K) and the triplet photoinduced absorption at 1.36 eV of figure 5 (10 K, open circles; 30 K, open squares; 50 K, open triangles); all for improved PPV. The luminescence signals at 30 and 50 K are identical to that at 10 K. The pump energy was 2.71 eV at less than 40 mW cm^{-2}.

5.2. *Photoconductivity results*

Figure 8 shows the photoconductivity action spectra of improved PPV (at two temperatures) together with the absorption spectrum of the same sample (note that these samples are not quite as well ordered, as gauged from the absorption spectrum, as those used for the absorption, luminescence, and photoinduced-absorption measurements reported above). The PPV is deposited on top of an Au interdigitated electrode array on quartz and the photoconductivity action spectrum was found to be the same for illumination from either side. The results shown here are all taken with illumination of the electrode-array side. The

spectrum in figure 8 is normalized to constant incident intensity, measured with a calibrated power meter on the sample spot. Reflection at the substrate front side, the electrodes, and the substrate back side/PPV interface (spectrally strongly varying) is not taken into account. We estimate a value of intensity absorbed in the sample of roughly 50 μW cm^{-2} at 2.7 eV for the action spectrum shown in figure 8. The photoconductivity response shows some sample variation and the actual power absorbed (even incident) is notoriously hard to estimate; therefore all values for excitation intensities given below are only rough estimates. Care has to be taken when interpreting the photoconductivity response in the absorption tail (below $\sim$ 2.2 eV). In this range the response is so small that effects due to thermal modulation of the dark conductivity may be significant.

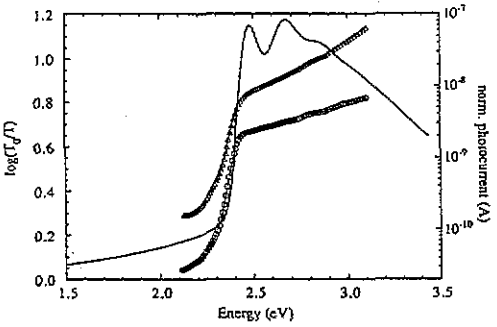

Figure 8. Optical absorption (full curve, left axis) and photoconductivity excitation spectrum (symbols, right axis) of improved PPV normalized to constant incident intensity (triangles, room temperature; circles, 250 K); applied electric field of 71 kV cm^{-1}. The intensity absorbed in the sample at 2.7 eV was roughly 50 μW cm^{-2}.

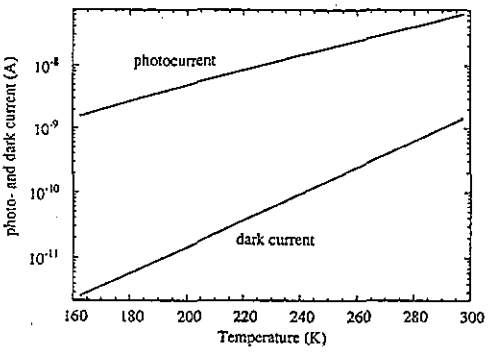

Figure 9. Temperature dependence of the dark current and photocurrent of improved PPV, both measured in steady-state condition, i.e. after saturation of the signals, with an excitation energy of 2.54 eV at around 100 μW cm^{-2} incident intensity, and an applied electric field of 100 kV cm^{-1}.

The action spectrum in figure 8 shows an onset of photoconductivity in the tail of the absorption spectrum, rising steeply up to about 2.4–2.45 eV, just below the $(0 \rightarrow 0)$ transition in absorption, and rising more weakly at higher energies. The form of the action spectrum is not strongly temperature dependent; at higher temperatures the photoconductivity response in the tail increases and the rise above the first absorption peak is slightly stronger. The ratio of photocurrent to dark current increases with decreasing temperature as the dark conductivity decreases more strongly on lowering the temperature.

We have measured the dependence of the photoconductivity response with excitation intensity I; we find a dependence as I^{α}, with $\alpha = 0.6$ for the improved PPV for excitation at 2.54 eV at room temperature in the range from about 0.25 to 500 μW cm^{-2} absorbed in the sample and at field strengths of up to 100 kV cm^{-1}. At 100 kV cm^{-1} at $\sim$ 500 μW cm^{-2} we observe an approximately 500-fold increase in current with respect to the dark current. There are various reports on steady-state photoconductivity in PPV [23, 52–56]. The sublinear response has been observed in some cases [53–55] and is close to the value of $\alpha = 0.5$ expected for bimolecular recombination. We note that high excitation densities, which favour bimolecular recombination, have been shown to be much more crucial in a surface-type sample geometry, which we have used here, as opposed to a sandwich cell [52]. This is due to the fact that both positive and negative charge carriers are created and move across

each other in the same plane parallel to the electric field and the film, giving rise to the 'bimolecular' intensity dependence.

This sublinear intensity response accounts for the differences in the action spectra between that reported here and those reported previously for standard PPV, where the photoconductivity has been observed to peak in the region of the absorption edge, falling strongly at increasing photon energies [23, 53, 56]. The difference between these and the present experiments is that we have used very much thinner PPV samples. Since the peak absorbance for the samples used in the present work is typically no higher than unity, the full sample thickness is excited at all energies above the band gap, and the action spectrum is unaffected by the sublinear intensity dependence. In contrast, for the thicker samples used previously [23, 53, 56], the confinement of the excitation to the surface region of the film for excitation above the bandgap increases the excitation density and, through the sublinear intensity dependence, causes a reduction in the photocurrent. It is thus expected that the photoconductivity response will peak on the rising edge of the absorption band, at the energy at which photons are absorbed through the full thickness of the sample. These issues can be investigated in more detail in PPV photodiode structures at different bias polarities [57].

We found that the temporal response of the photocurrent was dependent on the illumination intensity in a reproducible way. When we exposed the samples to low light levels (starting from about 0.25 μW cm^{-2} absorbed), we saw a strong instantaneous increase in current followed by a slow but continuous increase and a saturation of the photocurrent only after prolonged exposure (several minutes). On increasing the pump intensity, the photocurrent signal saturates more quickly, so that there is a pump intensity at which we observe a steep rise of the photocurrent with an almost instant saturation. On increasing the illumination intensity further (to levels above $\sim$ 400 μW cm^{-2} absorbed), the photocurrent signal actually drops slowly for some time after the initial steep rise. This effect provides a further indication of the importance of trap states and the possibility of the creation of significant concentrations of space charge, due to different mobilities of positive and negative charge carriers in PPV [58, 59].

Investigations of the electric field dependence of the photocurrent over a limited range of 10–100 kV cm^{-12} reveal a slight increase of the band-tail photoconductivity (below $\sim$ 2.35 eV) at higher applied electric fields, due to the electric-field-enhanced release of carriers from trap states. The photocurrent for excitation above the band edge increases slightly superlinearly with field. This may be due to the fact that the current/voltage characteristics of our samples were not perfectly ohmic; the dark current increases slightly superlinearly with voltage. There may be some slight difference in the slopes of the current/voltage characteristics for the sample in the dark and under illumination, which would (together with the not perfectly ohmic contacts) indicate the influence of interface-sensitized photoconductivity. These effects will be investigated in more detail.

As mentioned above, the photocurrent and the dark current decrease with decreasing temperature, more strongly so for the dark current. This is shown in figure 9, in which we observe an approximately 40-fold increase of the current by illumination at room temperature; this ratio increases to $\sim$ 600 at 160 K. The decrease in photocurrent and dark current on this semilogarithmic plot is almost linear over the whole temperature range shown. An Arrhenius plot of the photocurrent PC and the dark current DC, ln(1/DC) or ln(1/PC) versus reciprocal temperature, can therefore not give good fits. We have, however, calculated such fits for the range from room temperature to $\sim$ 250 K and obtain activation energies of about 0.16 eV for the photocurrent and about 0.31 eV for the dark current. The activation energy of 0.16 eV for the photocurrent is in good agreement with earlier reports on PPV and derivatives [52, 54].

Figure 10 shows the development of the photocurrent signal with time. In this experiment we have simply disabled all filtering and signal averaging of our source/measure unit. The time resolution is therefore only slightly better than 0.5 ms. Within this time resolution there is an instantaneous increase of the current upon light exposure. At the level of illumination of the sample in figure 9 the photocurrent saturates quickly. After the illumination is stopped the signal decays with fast and slow components. In the range of $\sim$ 10–100 kV cm^{-1} applied electric field we have not observed any significant changes in the temporal decay of the photocurrent after illumination.

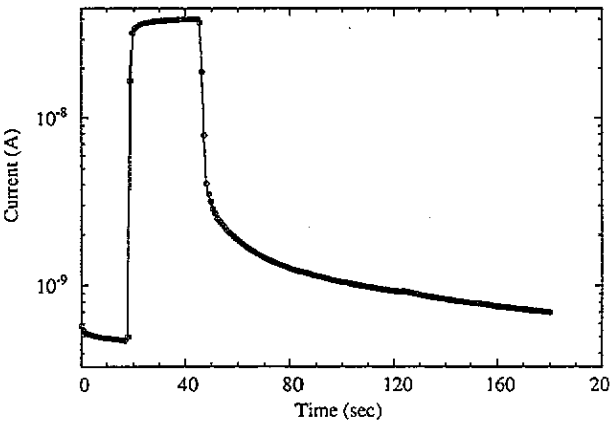

Figure 10. Development of the dark current and photocurrent in improved PPV with time. At $\sim$ 20 s the illumination was switched on; at $\sim$ 45 s the illumination was stopped. The pump energy was 2.54 eV and the incident pump intensity of the order of 50 μW cm^{-2}, at room temperature and an electric field of 71 kV cm^{-1}.

5.3. Discussion

5.3.1. Model for photoconductivity. The principal result that is established very clearly in the present work is that the photoconductivity onset coincides with the first peak in the absorption spectrum. This demonstrates that the photocarriers responsible for the photocurrent are generated through the creation of the photoexcitations produced at this absorption peak, which we identify in section 4 to be the (0 $\rightarrow$ 0) transition to the vibrationally relaxed state of the singlet exciton. We consider that charge carriers are produced through exciton ionization within the lifetime of the exciton (typically 250 ps [20]). We note therefore that in the limit, applicable here, where only a small fraction of excitations dissociate to form separated charges, the number of photocarriers produced will scale with the lifetime, τ of the exciton, and this will be longer in polymers with high luminescence efficiencies (the maximum exciton lifetime is achieved when decay occurs only through radiative channels). That there is no offset between the absorption edge and the photoconductivity onset does not require that the exciton has zero binding energy. Indeed, there are clear indications that the binding energy, E_B, for the singlet exciton in PPV, is about 0.4 eV, as assessed for example from the electric-field-induced quenching of the luminescence [60], and as obtained from recent theoretical studies [41]. Magnetic-field-dependence measurements of the photoconductivity in PPV have given a value of about 0.3 eV for E_B [42].

The field and temperature dependence of the photocurrent provide further information about the nature of the charge photogeneration and transport properties. Under steady-state conditions the photocurrent is a measure of the rate of generation of photoexcited charges, and is not sensitive to the carrier mobility. The activation energy for the photocurrent is 0.16 eV (at an electric field of 100 kV cm^{-1}), which is considerably smaller than for the

dark carriers (0.31 eV, also at 100 kV cm^{-1}), and is considerably less than 0.4 eV. We have observed similar behaviour for the short-circuit current in sandwich-structure photovoltaic cells made with PPV [57]. The activation energy is found there to be very dependent on the applied electric field, rising to 0.4 eV when the device is held at its open-circuit voltage (zero internal field), and we consider that the lower activation energy may result from electric-field-assisted lowering of the exciton ionization energy.

We do not consider that ionization requires that excitons migrate to the surface. Exciton diffusion ranges are not considered to be large in PPV (a value of 5 nm was estimated for poly(3-hexylthienylene) [61]), and diffusion over distances of up to 1 μm would be necessary to apply the analysis of the thickness dependence of the action spectrum presented in section 5.2. Very extensive work has been done on photoconductivity in the polydiacetylenes [3], which appear to behave very differently from PPV. In particular, the photoconductivity onset in the polydiacetylenes is displaced to considerably higher energies (> 0.5 eV) than the first excitonic absorption feature, and it is considered that the photoconductivity onset is at the energy required to ionize the exciton. The polydiacetylenes are different from PPV in two important respects: first, these materials are generally very much more anisotropic than PPV so that the three-dimensional motion of the charge carriers that we consider for PPV may not be appropriate for the polydiacetylenes, and secondly, the quantum yield for photoluminescence is very low, with facile non-radiative decay reducing the lifetime of the excited states to less than 2 ps [62]. Thus, the chances for exciton ionization are very much smaller than is the case for PPV.

5.3.2. Character of the photocarriers. The separated electrons and holes photogenerated in PPV are expected to thermalize as singly charged polarons or as doubly charged bipolarons. The latter have been identified in earlier measurements of photoinduced absorption in type-I standard PPV [16, 24], but are not seen in the PPV samples used in the present work. We consider that the bulk of the photocarriers should be of the same type as those injected from electrodes in the sandwich-structure electroluminescent diodes, LEDs, which we have investigated in detail [17, 18]. In these diodes, the majority of the injected carriers are believed to be present as singly charged polarons, which do not show induced absorption bands in accessible parts of the spectrum; the dominant induced absorption band should be very close in energy to the singlet luminescence, and bands in the infra-red are expected at wavelengths beyond 2.5 μm [61, 63]. The absence of the 'bipolaron' absorption bands in the photoinduced-absorption spectrum of PPV (figure 5) is consistent with the information available from the LEDs: measurements of induced absorption obtained under forward bias of the LEDs shows both a strong response at the triplet–triplet transition energy ($\sim$ 1.4 eV), and also a weaker pair of features at 0.6 and 1.6 eV which are identified as the 'bipolaron' transitions seen in the photoinduced absorption of type-I standard PPV [17]. Analysis of the size of these induced-absorption bands shows that these 'bipolarons' are present in the LEDs as a very minor fraction of the injected charges, and it is considered that these states are defect stabilized, and formed much more easily under the conditions of net space charge that are present in the LEDs. A net space charge is absent in the photoinduced-absorption experiment. We briefly mention here that the observation or absence of photoinduced 'bipolaron' bands in oligomers and various derivatives of PPV depends very much on the precise nature (e.g. morphology, defect concentration, etc) of the materials and that these issues are discussed in more detail elsewhere [5–7].

We therefore identify the charge carriers generated under the conditions used in the induced-absorption and photoconductivity experiments as polarons. We note that hole polarons are considered to be very much more mobile than electron polarons in PPV

[58, 59, 64]. We consider that the more rapid photoconductivity response is due to hole polarons, and that the longer-time-scale response is associated with electron polarons.

6. Conclusion

The results presented here on the photophysics of PPV prepared with a high level of intrachain order demonstrate that disorder at relatively long length scales can have a very strong influence on the energetics and dynamics of both charged and neutral photoexcitations. This highlights the importance of disorder in determining the semiconductor physics of conjugated polymers.

Acknowledgments

We would like to thank R Jackson for the preparation of some of the standard PPV used in this study. We are grateful for financial support from the Commission of European Communities programme CEC-BRITE/EURAM (Basis Research in Industrial Technologies for Europe/European Advanced Materials) contract 0148—project NAPOLEO (Nouvelles Applications de Polymères à l'Electronique et à l'Optique). We also thank the Science and Engineering Research Council and the Nuffield Foundation (RHF) for support.

References

[1] 1993 *Proc. Int. Conf. on the Science and Technology of Synthetic Metals (Gothenburg, 1992); Synth. Met.* **55–57**
[2] Skotheim T (ed) 1986 *Handbook of Conducting Polymers* vols 1 & 2 (New York: Dekker)
[3] Bloor D and Chance R R (ed) 1985 *NATO ASI Series E, No 102* (Dordrecht: Martinus Nijhoff)
[4] Townsend P D and Friend R H 1987 *J. Phys. C: Solid State Phys.* **20** 4221
[5] Woo H S, Graham S C, Halliday D A, Bradley D D C, Friend R H, Burn P L and Holmes A B 1992 *Phys. Rev.* B **46** 7379
[6] Woo H S, Lhost O, Graham S C, Bradley D D C, Friend R H, Quattrocchi C, Bredas J L, Schenk R and Müllen K 1993 *Synth. Met.* **59** 13
[7] Smilowitz L and Heeger A J 1992 *Synth. Met.* **48** 193
[8] Pichler K and Leising G 1990 *Europhys. Lett.* **12** 533
[9] Burroughes J H, Bradley D D C, Brown A R, Marks R N, McKay K, Friend R H, Burn P L and Holmes A B 1990 *Nature* **347** 539
[10] Burn P L, Bradley D D C, Friend R H, Halliday D A, Holmes A B, Jackson R W and Kraft A 1992 *J. Chem. Soc. Perkin Trans.* 3225 and references therein
[11] Halliday D A, Burn P L, Bradley D D C, Friend R H, Gelsen O, Holmes A B, Kraft A, Martens J H F and Pichler K 1993 *Adv. Mater.* **5** 40
[12] Halliday D A, Burn P L, Friend R H, Bradley D D C, Holmes A B and Kraft A 1992 *Synth. Met.* **55–57** 954
[13] Pope M and Swenberg C 1982 *Electronic Processes in Organic Crystals* (Oxford: Clarendon)
[14] Heeger A J, Kivelson S, Schrieffer J R and Su W P 1988 *Rev. Mod. Phys.* **60** 781
[15] Baeriswyl D, Campbell D K and Mazumdar S 1992 *Springer Series in Solid State Sciences 102* ed H G Kiess (Berlin: Springer)
[16] Colaneri N F, Bradley D D C, Friend R H, Burn P L, Holmes A B and Spangler C W 1990 *Phys. Rev.* B **42** 11 670
[17] Brown A R, Pichler K, Greenham N C, Bradley D D C, Friend R H and Holmes A B 1993 *Chem. Phys. Lett.* **210** 61
[18] Swanson L S, Shinar J, Brown A R, Bradley D D C, Friend R H, Burn P L, Kraft A and Holmes A B 1992 *Phys. Rev.* B **46** 15 072

[19] Swanson L S, Lane P A, Shinar J and Wudl F 1991 *Phys. Rev.* B **44** 10617
[20] Samuel I D W, Crystall B, Rumbles G, Burn P L, Holmes A B and Friend R H 1992 *Synth. Met.* **54** 281
[21] Kersting R, Lemmer U, Mahrt R F, Leo K, Kurz H, Bässler H and Göbel E O 1993 *Phys. Rev. Lett.* **70** 3820
[22] Hagler T W, Pakbaz K, Voss K F and Heeger A J 1991 *Phys. Rev.* B **44** 8652
[23] Fukuda T, Kubo T, Takezoe H and Fukuda A 1992 *Japan. J. Appl. Phys.* **31** 67
[24] Wei X, Hess B C, Vardeny Z V and Wudl F 1992 *Phys. Rev. Lett.* **68** 666
[25] Tian B, Zerbi G and Müllen K 1991 *J. Chem. Phys.* **95** 3198
[26] Tian B, Zerbi G, Schenk R and Müllen K 1991 *J. Chem. Phys.* **95** 3191
[27] Heun S, Mahrt R F, Greiner A, Lemmer U, Bässler H, Halliday D A, Bradley D D C, Burn P L and Holmes A B 1993 *J. Phys.: Condens. Matter* **5** 247
[28] Rauscher U, Schütz L, Greiner A and Bässler H 1989 *J. Phys.: Condens. Matter* **1** 9751
[29] Martens J H F, Halliday D A, Marseglia E A, Bradley D D C, Friend R H, Burn P L and Holmes A B 1993 *Synth. Met.* **55–57** 434
[30] Lhost O and Bredas J L 1992 *J. Chem. Phys.* **96** 5279
[31] Chen D, Winokur M J, Masse M A and Karasz F E 1992 *Polymer* **33** 3116
[32] Mao G, Fischer J E, Karasz F E and Winokur M J 1993 *J. Chem. Phys.* **98** 712
[33] Simpson J H, Rice D M and Karasz F E 1991 *Polymer* **32** 2340
[34] Simpson J H, Rice D M and Karasz F E 1992 *J. Polym. Sci. Polym. Phys.* **30** 11
[35] Rauscher U, Bässler H, Bradley D D C and Hennecke M 1990 *Phys. Rev.* B **42** 9830
[36] Fesser K, Bishop A R and Campbell D K 1983 *Phys. Rev.* B **27** 4804
[37] Bässler H, Gailberger M, Mahrt R F, Oberski J M and Weiser G 1992 *Synth. Met.* **49–50** 341
[38] Binh N T, Gailberger M and Bässler H 1992 *Synth. Met.* **47** 77
[39] Binh N T, Minh L Q and Bässler H 1993 *Synth. Met.* **58** 39
[40] Smilowitz L, Hays A, Heeger A J, Wang G and Bowers J E 1992 *J. Chem. Phys.* **98** 6504
[41] Gomes da Costa P and Conwell E M 1993 *Phys. Rev.* B **48** 1993
[42] Frankevich E L, Lymarev A A, Sokolik I, Karasz F E, Blunstengel S, Baughman R H and Hörhold H H 1992 *Phys. Rev.* B **46** 9320
[43] Friend R H 1993 *Proc. Nobel Symp. on Conjugated Polymers and Related Materials (Lulea, 1991)* ed W R Salaneck, I Lundström and B Rånby (Oxford: Oxford University Press) pp 285–323
[44] Vogl P and Campbell D K 1989 *Phys. Rev. Lett.* **62** 2012
[45] Mizes H A and Conwell E M 1993 *Phys. Rev. Lett.* **70** 1505
[46] Burn P L, Bradley D D C, Brown A R, Friend R H, Halliday D A, Holmes A B, Kraft A and Martens J H F 1992 *Springer Series in Solid State Sciences 107* (Berlin: Springer) p 293
[47] Pichler K, Friend R H, Burn P L and Holmes A B 1993 *Synth. Met.* **55–57** 454
[48] Stenger-Smith J D, Lenz R W and Wegner G 1989 *Polymer* **30** 1048
[49] Yoshimura T, Tatsuura S, Sotoyama W, Matsuura A and Hayano T 1992 *Appl. Phys. Lett.* **60** 268
[50] Hagler T W, Pakbaz K, Moulton J, Wudl F, Smith P and Heeger A J 1991 *Polym. Commun.* **32** 339
[51] Gomes da Costa P, Dandrea R G and Conwell E M 1993 *Phys. Rev.* B **47** 1800
[52] Gailberger M and Bässler H 1991 *Phys. Rev.* B **44** 8643
[53] Tokito S, Tsutsui T, Tanaka R and Saito S 1986 *Japan. J. Appl. Phys.* **25** L680
[54] Obrzut J, Obrzut M J and Karasz F E 1989 *Synth. Met.* **29** E103
[55] Lee C H, Yu G and Heeger A J 1992 *Phys. Rev.* B **47** 15543
[56] Takiguchi T, Park D H, Ueno H, Yoshino K and Sugimoto R 1987 *Synth. Met.* **17** 657
[57] Marks R N, Halls J M *et al* in preparation
[58] Antoniadis H and Abkowitz M A private communication
[59] Marks R N private communication
[60] Hamer P *et al* in preparation
[61] Ziemelis K E, Hussain A T, Bradley D D C, Friend R H, Rühe J and Wegner G 1991 *Phys. Rev. Lett.* **66** 2231
[62] Kobayashi T, Yoshizawa M, Stamm U, Taiji M and Hasegawa M 1990 *J. Opt. Soc. Am.* B **7** 1558
[63] Harrison M G, Ziemelis K E, Friend R H, Burn P L and Holmes A B 1992 *Synth. Met.* **55–57** 218
[64] Brown A R, Greenham N C, Burroughes J H, Bradley D D C, Friend R H, Burn P L, Kraft A and Holmes A B 1992 *Chem. Phys. Lett.* **200** 46